Artificial Recognition Sorbents on Multiwalled Carbon Nanotubes for the Separation of Aspirin from its Structural Analogues

Sooraj. M.P, Beena Mathew*
School of Chemical Sciences, Mahatma Gandhi University, Kottayam, 686560, Kerala, India
*e-mail: beenamscs@gmail.com, Telephone No: (+91) – 481 – 2731036, Fax: (+91) – 481 – 2731036

ABSTRACT: Highly specific and selective artificial recognition units for aspirin was fabricated on polymer-nanocomposites (MWCNT-MIP) making use of molecular imprinting technology. The products were characterised using Fourier-transform infrared spectroscopy, powder X-Ray diffraction studies, thermogravimetric analysis, scanning electron microscopic and tunnelling electron microscopic techniques. The maximum saturated binding capacity (Qmax) for MWCNT-MIP was obtained as 0.644mmolg-1 with an 82% increase as compared with the non-imprinted counterpart (MWCNT-NIP). MWCNT-MIP shows a high regression coefficient value (R2=0.999) for Langmuir adsorption isotherm indicating enhanced homogeneity than the corresponding bulk MIP (R2=0.977). The rebinding process obeys second order kinetics with rapid template binding demonstrating the effective formation of print cavities on the surface of sorbent. Also, the theoretical and experimental values for Qe from second order kinetic data were found to be almost similar even at different temperatures. The optimized rebinding parameters of the nanosorbents were applied for the separation of aspirin from its closely related structural analogues and these studies indicated a higher relative selectivity coefficient for MWCNT-MIP towards aspirin than the bulk MIP. Further MWCNT-MIP is found to have 100% reproducibility upto four adsorption-desorption cycles.

KEYWORDS: molecular imprinting; multiwalled carbon nanotubes; selective recognition; regeneration; aspirin; specificity

IJSER

INTRODUCTION

Molecular imprinting is a method to synthesize artificial receptor materials with sites of high specificity and selectivity towards the target molecules. Optimum amount of crosslinker helps to maintain the rigidity of the polymer and its well defined recognition sites [1]. The molecularly imprinted polymer (MIP) retains its template rebinding capacity because of its functional arrangement regarding shape selectivity and pre-organisation of functional groups [2]. Because of their molecular rebinding ability, stability under different circumstances, cost-effectiveness and ease of synthesis, MIPs have been used in wide varieties of applications such as separation science [3,4] sensing[5,6] and drug delivery[7]. The difficulties faced by the conventional bulk molecular imprinted polymers are deeply buried cavities, formation of heterogeneous binding sites, and entrapment of template molecules in the polymer matrix leading to poor site accessibility [8] etc. It would reduce the kinetics of binding target analyte and increase the heterogeneity of MIPs.

Carbon nanotubes (CNTs) have been of great interest right from their discovery [9], because of their many a unique properties. It is already proved that CNT is a very good support material for molecularly imprinted polymers [10]. After the incorporation of CNTs the polymer matrix shows increased surface to volume ratio [11]. Here the imprinted polymers wrap around the CNTs and eventually, most of the cavities are near or in the surface, with most template molecules being removed from the highly cross-linked matrix.

Aspirin (o-acetyl salicylic acid, hitherto abbreviated as ASP) is an analgesic and antipyretic agent, widely used in pharmaceutical formulations for the relief of headaches, fever etc [12]. Many methods have already been reported for the detection and separation of ASP from its structurally related compounds but with minimum separation ability and slow kinetics [13]. We present here a highly specific and efficient novel nanostructure sorbent having faster kinetics for the selective recognition and separation of ASP from its structural analogues based on imprinting technology.

The molecularly imprinted sorbent was prepared on multiwalled carbon nanotubes (MWCNT-MIP) with ASP as template, 1-vinylimdazole (VIZ) as functional monomer, ethylene glycol dimethacrylate (EGDMA) as cross-linker and azobisisobutyronitrile (AIBN) as initiator. The selective recognition of MWCNT-MIP/MIP towards ASP molecule was evaluated using adsorption experiments. The adsorption isotherms and adsorption kinetics of the sorbents were also studied in detail. The product and intermediates formed during the synthesis of MWCNT-MIP were analyzed using FT-IR, powder XRD and thermo gravimetric analyses and their morphologies were observed using scanning electron microscopy and TEM techniques.

EXPERIMENTAL

Materials

Multiwalled carbon nanotube (MWCNT) was purchased from Reinste Nano Ventures Private Limited, India. VIZ (98%), 2-hydroxy ethyl methacrylate (HEMA, 98%), EGDMA (98%) and all solvents (HPLC grade) were obtained from Merck India. ASP (99%), salicylic acid (SA, 99%), benzoic acid (BA, 99%), AIBN and thionylchloride ($SOCl_2$) were obtained from Sigma Aldrich. All the chemicals and solvents were used without further purification. Doubly distilled water was used throughout the course of the experiments as and when required.

Apparatus

Fourier-transform infrared (FT-IR) spectrum was recorded on a Perkin-Elmer spectrum 400 FT-IR spectrophotometer in the range 4000 to 400 cm^{-1}. Ultraviolet-visible (UV–vis) absorption spectra were investigated on a Shimadzu UV-vis spectrophotometer model 2450 using chloroform as solvent. Thermo gravimetric analysis (TGA) was conducted on a NETZSCHSTA449C instrument from room temperature to 800^{o}C at a constant heating rate of 10^{o}C under an inert atmosphere. Morphological images were recorded on a JEOL-JSM-6390A scanning electron microscope (SEM) and JEOL-2100 model tunneling electron microscope (TEM). The centrifugations were done on a laboratory centrifuge, Remi **R-12M model.** The chemical structures were generated from CS ChemDraw Pro 8.0 and the graphs were plotted using OriginPro 8 software package.

Preparation of vinyl functionalized MWCNT (MWCNT-CH=CH_2)

The purified [14] MWCNT (100mg) was taken in a round bottom flask, 50mL conc. HNO_3 was added followed by sonication for about 15 minutes in a bath type sonicator at 40 KHz. The reaction flask was then put into an oil bath maintained at 80^{o}C equipped with a reflux condenser for 7.5h under vigorous stirring. The mixture was then diluted with excess amount of deionised water and filtered through 0.2μm PTFE membrane to separate the solid components. Washing was repeated until pH of the

filtrate became neutral. The obtained solid product was dried under vacuum at 60°C for 24 hours, yielding MWCNT with carboxyl functionalization. 250mg of MWCNT-COOH and 10mL of $SOCl_2$ in 15mL THF were taken in a reaction flask equipped with reflux condenser. The reaction mixture was refluxed at 65°C for 24h under vigorous stirring. After cooling, the mixture was repeatedly washed with THF (5x25mL). The solid product was separated from THF solution through centrifugation at 14000 rpm which was then dried under vacuum at 60°C for 18h. Vinyl functionalization of MWCNT-COCl was done using 3mL 2-hydroxy ethylmethacrylate [15].

Preparation of aspirin (ASP) molecularly imprinted polymer on MWCNT (MWCNT-MIP)

0.075g of vinyl functionalized MWCNT was mixed with 0.5mmol of 1-vinylimidazole (VIZ), 0.1mmol ASP and 1mmol EGDMA in a reaction vessel equipped with a reflux condenser containing 25mL chloroform. For better dispersion the mixture was soniccated for 20min. To this, 50mg of the initiator AIBN was added and refluxed at 70°C for 24 hours under N_2 atmos. The separated polymer was ground well and washed repeatedly with chloroform with constant monitoring using UV-vis. spectroscopy (λ_{max}=276nm) for the complete removal of ASP molecules from the polymer matrix (figure 1). The obtained polymer was dried under vacuum for 24h before use. For comparison, the non-imprinted polymers on MWCNT (MWCNT-NIP) were also prepared using the same procedure, but without using the drug molecules in the polymerization process.

Preparation of bulk polymers (MIP/NIP)

The conventional bulk MIP and NIP were prepared as discussed above; but in the absence of MWCNTs.

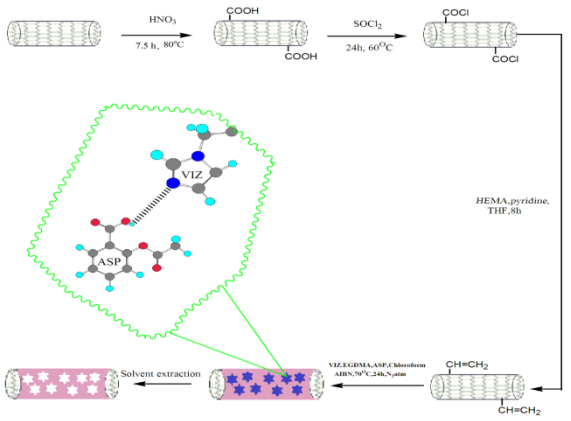

Fig. 1 Synthesis route of MWCNT-MIP

Concentration study

10mg of MWCNT-MIPs/NIPs were batch equilibrated with 8mL of ASP solution having varying concentration (0.4 to 4mmolL^{-1}). The mixture was then centrifuged to separate the sorbent. Concentration at which maximum amount of ASP bound by the polymer was determined using the equation:

$$Q_e = (C_o - C_e)V/M \ldots\ldots\ldots\ldots (1)$$

where C_o (mmolL^{-1}) and C_e (mmolL^{-1}) are the initial and equilibrium concentration, V (L) is the volume of aspirin solution and M (g) is the weight of the sorbent. The experiment was repeated for bulk MIPs/NIPs also.

Study on the effect of sorbent mass

5, 10, 15 and 20mg of MWCNT-MIP/NIP and MIP/NIP were added to the optimum concentration of ASP solution (4mmolL^{-1}) and shaken for 4h. The amount of ASP bound by the sorbents was calculated using equation (1).

Adsorption isotherm study

10mg of the imprinted sorbents were added to 8mL each of template solution having different concentration ranging from 0.4 to 4mmolL^{-1}. After 4h equilibration the mixture was centrifuged and decanted. From UV-vis. absorption data at λ_{max} = 276nm, concentration of the supernatant liquid and the adsorption capacity (Q_e) of the adsorbent was calculated (eqn 1). The theoretical adsorption capacity value for the adsorbent was also calculated using the Langmuir (2) and Freundlich (3) equations:

$$(1/Q_e) = (1/Q_m) + (1/Q_m K_a)\ x\ (1/C_e) \ldots\ldots\ldots (2)$$

$log\ (Q_e) = log\ K_F + 1/n\ log\ C_e$…….....(3)

where C_e (mmolL^{-1}) and Q_e (mmolg^{-1}) are ASP concentration and amount adsorbed at adsorption equilibrium, Q_m (mmolg^{-1}) and K_a (Lmmol^{-1}) are the theoretical maximum adsorption capacity and Langmuir equilibrium constant related to the theoretical maximum adsorption capacity and energy of adsorption, respectively. K_F ((mmol/g)(L/mmol)$^{1/n}$) and n are the Freundlich constants, which indicate the adsorption capacity and adsorption intensity, respectively. The parameters of each model found from the slope and intercept of different plots were compared using regression analysis.

Kinetic studies

Batch equilibration process was used for the kinetic studies. A number of 8mL samples of 4mmolL^{-1} ASP solution were treated with 10mg of MWCNT-MIP. At different time intervals, the sorbents were separated from the solution by centrifugation (1600rpm), filtered and determined concentration of ASP in the supernatant at 276nm using a UV-vis. spectrophotometer. The amount of template bound at different time intervals was calculated using equation (1).

The sorption kinetic data was analyzed using the Langergen first order rate model [16]. The equations involved are as below:

$dQ_t/d_t = k_1(Q_e - Q)$ ……..(4)

where k_1 (min^{-1}) is the rate constant of pseudo-first-order sorption, Q_t denotes the amount of ASP sorption (mmolg^{-1}) at time t (min) and Q_e denotes the amount of ASP adsorption (mmolg^{-1}) at equilibrium. After definite integration and applying the initial conditions $Q_t = 0$ at $t = 0$ and $Q_t = Q_t$ at $t = t$, equation (1) becomes:

$ln(Q_e - Q_t) = ln(Q_e) - k_1 t$ ……(5)

In addition, a pseudo-second-order equation proposed by Ho and McKay [17] based on the assumption that the adsorption follows chemisorption may be expressed in the form:

$dQ_t/d_t = k_2(Q_e - Q)^2$ ……..(6)

where k_2 is the rate constant of pseudo-second-order sorption. Integrating equation (3) and applying the initial conditions,

$1/(Q_e-Q_t) =(1/Q_e) + k_2 t$ ……(7)

or equivalently

$(t/Q_t) =(1/k_2 Qe^2) + t/Q_e$ .....(8)

From the plots $ln(Q_e-Q_t)$ vs t and t/Q_t vs t the values of maximum amount of template bound at equilibrium (Q_e) and corresponding rate constants were calculated.

Selectivity studies

The selectivity studies of the imprinted polymers towards aspirin (ASP) and its structural analogues salicylic acid (SA) and benzoic acid (BA) were done using 4mmolL^{-1} solution under batch equilibration process. The procedure was same as that of adsorption studies. The extent of selectivity inherently depends on the number and complimentarity of the imprinted cavities and also their rebinding ability; this effect was calculated using the equation:

$K_d = (C_i-C_f)V/MC_f$ ……(9)

where K_d (Lg^{-1}) is the distribution coefficient, C_i (mmolL^{-1}) and C_f (mmolL^{-1}) are the initial and final solution concentrations respectively, V (L) is the volume of the solution and M (g), the mass of sorbent used.

The selectivity coefficient (k) and relative selectivity coefficient (k') were determined using equations (7) and (8):

$k = K_{template}/K_{analogue}$ ……(10)

$k' = K_{MIP}/K_{NIP}$ ……(11)

Reusability

The reusability of the synthesized MIPs was checked using batch equilibration method. 10 mg each of MWCNT-MIP and bulk MIP polymers were weighed and incubated in 8mL solutions of ASP having optimum concentration (4mmolL^{-1}). After 4h of incubation, the polymers were separated and the amount of bound ASP was analyzed from the supernatant liquid by UV-vis. spectroscopy. The polymers were washed with chloroform and dried under vacuum for the next application. The experiments were repeated 6 times using the same polymers under the same conditions.

RESULTS AND DISCUSSION

FTIR spectra were used to analyse the functionality changes of all intermediates and products. Figure 2 shows the FTIR spectra of purified, acid and vinyl functionalized carbon nanotubes and MWCNT-MIP with and without ASP. In the spectrum of purified MWCNT (a), a strong band at 1737 cm^{-1} corresponds

IJSER

to the C=O stretching vibration, while the peak at 2928 cm^{-1} corresponds to the asymmetric stretching vibration of C-H. The spectrum of acid processed MWCNTs (b) showed new peaks at 3300 and 1581 cm^{-1}, which confirmed the presence of –OH and –COOH functional groups. The peak at 1352 cm^{-1} could be attributed to the C–O stretching vibrations of –COOH. Spectrum of vinyl functionalized MWCNT (c) showed a strong peak associated with ether linkage around 1166 cm^{-1}. The presence of this peak suggests that HEMA is coupled to MWCNT through the -O- atom. MWCNT-MIP before and after washing demonstrates some notable changes in their spectra. First case showed shorter and broader peaks around 3300-2500 cm^{-1} representative of the -OH stretching of the carboxylic acid in aspirin [18]. The peaks at 1682 and 1750 cm^{-1} are due to the carboxylic acid carbonyl stretching and the carbonyl stretching of the ester unit of ASP respectively. All these point out to the embedding of ASP within the nanostructured sorbents.

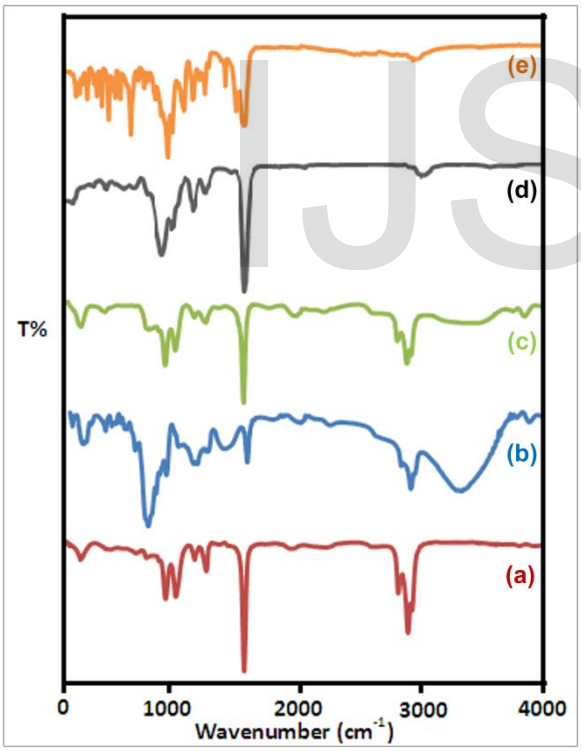

Fig. 2 FTIR spectra of (a) purified MWCNT, (b) MWCNT-COOH, (c) MWCNT-CH=CH_2, (d) MWCNT-MIP after washing (e) before washing

The X-ray diffractogram of MWCNT showed two crystalline peaks at 2θ = 25.8° and 2θ = 43.7° due to the presence of hexagonal graphitic structure (Figure 3). The crystallinity of MWCNT was not affected by acid functionalisation as is seen from its PXRD pattern. Normal polymers scatter X-ray beams completely thereby giving broad peaks which was observed in the case of bulk MIP samples at 2θ = 15° that implies its amorphous nature. But the nanostructure-incorporated MIP showed the two sharp peaks characteristic of MWCNT with less intensity, in addition to the broad peaks of MIP. This also showed the effective incorporation of MWCNT into the polymer matrix.

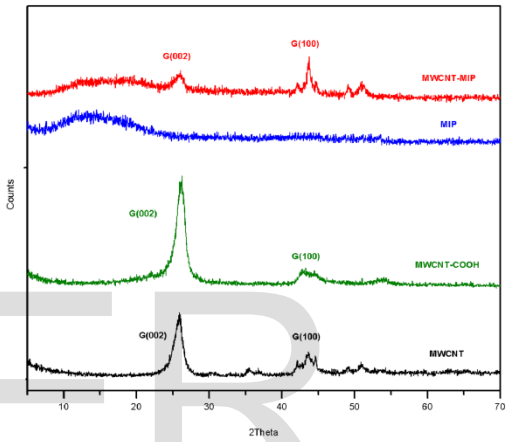

Fig. 3 Powder x-ray diffraction pattern of (a) MWCNT, (b) MWCNT-COOH, (c) MIP (d) MWCNT-MIP

Comparison of the thermal behavior of MWCNT, MWCNT-MIP and bulk MIPs were carried out by thermogravimetric analysis (Figure 4). Thermal degradation pattern of purified MWCNT was linear without any loss in mass up to 800°C. MWCNT-COOH showed a continuous weight loss but not in a huge amount (8%) due to the elimination of carbonyl groups from the surface of MWCNT. MWCNT-MIP showed a similar degradation pattern to that of pure MIP. Initially there was a small dip in the TGA curve of both MIPs corresponding to the removal of solvent molecules trapped inside the polymer matrix. The degradation temperature and mass loss were lower and higher respectively for MIP than MWCNT-MIP which indicates the greater thermal stability induced by the clubbing of MWCNT to the MIP. The difference in residual mass of bulk and nanostructured MIP showed that 12% of the initial weight of MWCNT-MIP comprised of multiwalled carbon nanotubes.

IJSER

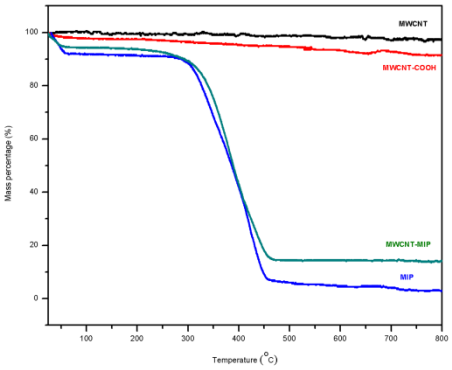

Fig. 4 TGA curves of (a) MWCNT, (b) MWCNT-COOH, (c) MWCNT-MIP (d) MIP

Purified MWCNTs showed tubular morphology in the SEM micrographs (Figure 5). After acid functionalisation, the morphology was found to be retained with a very slight increase in diameter. Bulk MIP showed a coagulated structure due to the agglomeration of polymer matrices. However the incorporation of nanomaterials into the molecularly imprinted polymer led to an entirely different morphology for MWCNT-MIP. For further clarification on the morphologies of the imprinted sorbents HR-TEM technique was made use of.

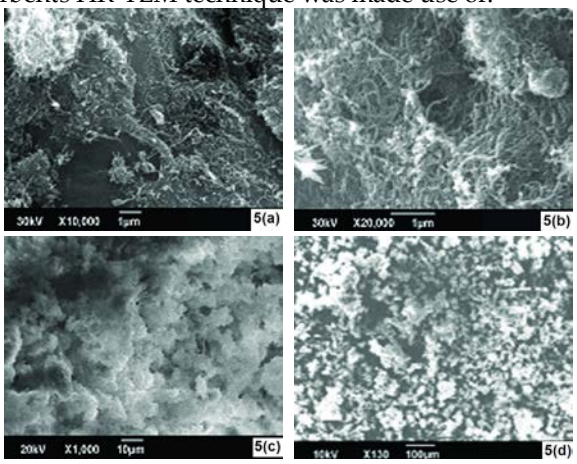

Fig. 5 SEM images of (a) MWCNT, (b) MWCNT-COOH (c) MIP (d) MWCNT-MIP

Concentration study

Figure 6 shows the effect of initial ASP concentration in the range of 0.4 to 4 mmolL^{-1}on adsorption by the imprinted and non-imprinted polymers. It was observed that the adsorption capacity increased (from 0.3058 to 0.6442mmolg^{-1}) for MWCNT-MIP and MIP (from 0.0710 to 0.5400mmolg^{-1}) with an increase in initial template concentration and attains equilibrium at 4mmolL^{-1}. The adsorption capacity of MWCNT-MIP was 16.17% higher than that of bulk MIP. The varying amount of adsorbance of ASP between MWCNT-MIP and MIP was caused by the difference in the number of available binding sites. Also the incorporation of nanostructures into the polymer matrix results in increased polymer-template surface of contact thereby providing higher valid collisions between the binding sites and template molecules. The increased affinity of the imprinted polymers towards the template molecule as compared to the non-imprinted polymers revealed the formation of template-complementary cavities in the imprinted polymers.

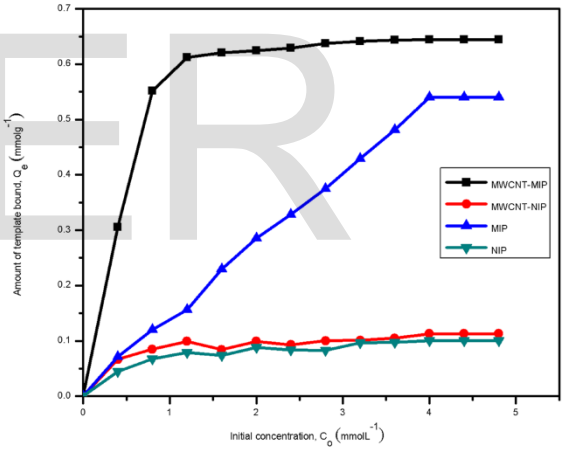

Fig. 6 Adsorption isotherms of imprinted and non-imprinted polymers (Amount of polymer 10mg; volume 8.0 mL; concentration of ASP from 0.4 to 4mmolL^{-1}

Adsorbent Dosage

Figure 7 presents the influence of varying adsorbent dosages on template sorption. The removal efficiency was found to increase with increase in sorbent dosage owing to the increase in number of binding sites. Further, MWCNT-MIP showed much greater removal efficiency due to the presence of increased surface 'memory cavities' which were deeply-set in the case of bulk MIP. Also, due to the absence of these specific binding sites, both the NIPs showed a

much less marked difference in the amount of ASP adsorbed.

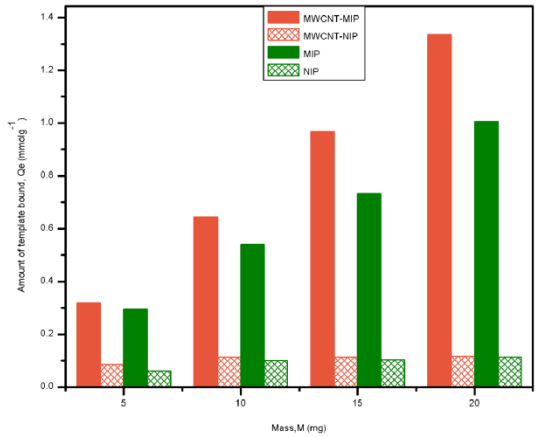

Fig. 7 Effect of adsorbent dosage on template bound (Amount of polymer varies from 5 to 20mg; volume, 8.0 mL; concentration of ASP, 4mmolL^{-1}, binding time 4h)

Adsorption isotherms

Adsorption isotherm data of MWCNT-MIP was well fit with the Langmuir model (Figure 8) whereas the non-nano MIPs fitted with Freundlich model (Figure 9), based on the least square fit method. A linear plot with R^2 value 0.999 was obtained from Langmuir adsorption isotherm for MWCNT-MIP, demonstrating that the adsorption process was mainly monolayer on a homogeneous adsorbent surface. The Langmuir constants Q_m and K_a were found to be 0.642 mmolg^{-1} and 51.378 Lmmol^{-1}, respectively. Also, the experimental (0.644mmolg^{-1}) and theoretical (0.642 mmolg^{-1}) maximum adsorption capacities towards ASP were found to substantiate the Langmuir model for MWCNT-MIP. The calculated isotherm constants and the corresponding correlation coefficients for MWCNT-MIP and MIP are shown in Table 1. The equilibrium data were further analyzed using the linearized form of Freundlich isotherm by plotting lnQ_e versus lnC_e, as shown in Figure 9. The theoretical and experimental values of the Freundlich isotherm show a large deviation in the case of MWCNT-MIP, while those for the Langmuir isotherm do not. However, bulk MIPs were found to obey Freundlich adsorption isotherm (R^2 = 0.990) thus evidencing its heterogeneous binding sites and multilayer adsorption.

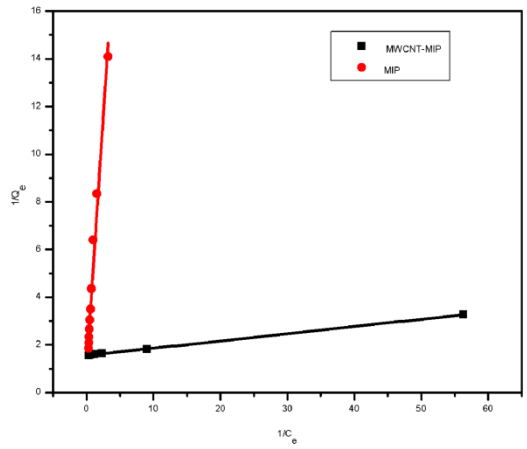

Fig. 8 Langmuir plot for adsorption of ASP by MWCNT-MIP and MIP (Amount of polymer 10mg; volume 8.0 mL; concentration of ASP 0.4 to 4mmolL^{-1}, binding time 4h)

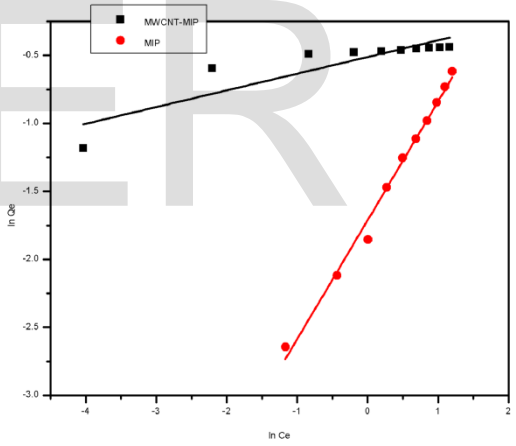

Fig. 9 Freundlich plot for adsorption of ASP by MWCNT-MIP and MIP (Amount of polymer, 10mg ; volume, 8.0 mL; concentration of ASP 0.4 to 4mmol L^{-1}, binding time 4h)

Adsorption Kinetics

The kinetic studies at different temperatures showed that the rapid adsorption of ASP occurred onto the recognition sites of MWCNT-MIP initially but slowed down with time (Figure 10). The maximum adsorption occurred after 1.5h at a capacity around 0.644mmolg^{-1}. The initial rapid adsorption occurs due to the availability of more binding sites on the surface of the sorbent which on forming non-covalent interactions with the template molecules

IJSER

becomes unavailable for further template binding thereby decreasing the rate of adsorption.

Pseudo-first and pseudo-second-order equations have been used for testing the kinetic data. In the case of pseudo-first-order equation, the constants were experimentally determined by plotting $ln(Q_e - Q_t)$ versus t (Figure 11) and are listed in Table 2. The low correlation coefficient indicated the first order kinetic model as less appropriate. The theoretical values (Q_e *cal*) exhibited larger deviations from experimental data (Q_e *exp*) (Table 2), again implying that the adsorption process does not follow fully the pseudo-first-order adsorption rate expression. The plot t/Q_t versus t (Figure 12) gave a straight line ($R^2 = 0.999$) suggesting that second order kinetics is applicable and from the slope and intercept of the plot, Q_e and k_2 were calculated respectively. Even as the temperature changes, the experimental and theoretical values for the amount of template bound (Q_e) were found to be compatible. These results authenticated that the second-order kinetic equation provided a better estimation as compared to the first-order kinetic equation. When the temperature was increased, values of kinetic parameters (k_2 and Q_e) decreased, showing that the process of adsorption was exothermic and the increased temperature resulted in the desorption of the template molecule from the adsorption sites [19].

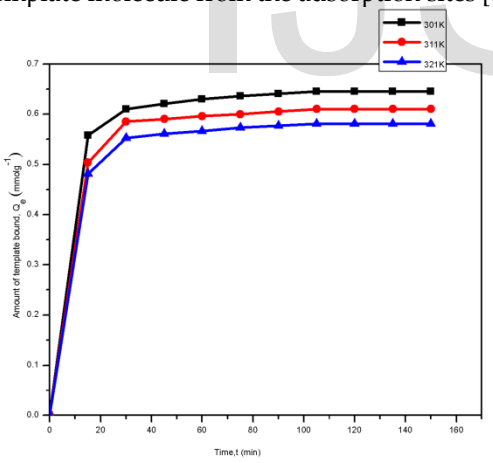

Fig.10 Adsorption rate of ASP by MWCNT-MIP (Amount of polymer 10mg; volume, 8.0 mL; concentration of ASP 0.4 to 4 4mmolL^{-1}, binding time 4h, temperature ranging from 301K to 321K)

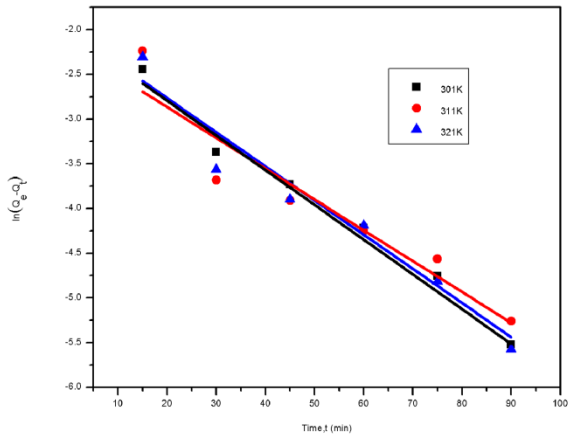

Fig. 11 First order kinetic plot for adsorption of ASP by MWCNT-MIP and MIP (Amount of polymer 10mg; volume 8.0 mL; concentration of ASP 4 mmolL^{-1}, binding time 4h, temperature ranging from 301K to 321K)

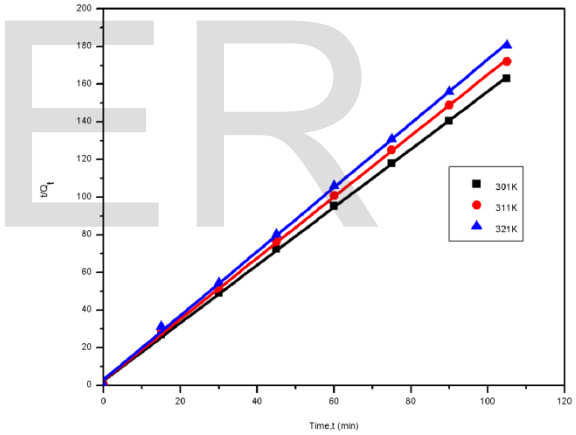

Fig. 12 Second order kinetic plot for adsorption of ASP by MWCNT-MIP and MIP (Amount of polymer 10mg; volume 8.0 mL; concentration of ASP 4mmolL^{-1}, binding time 4h,temperature ranging from 301K to 321K)

Selectivity studies

To check the selectivity of MWCNT-MIP, MIP and non-imprinted polymers of both sorbents towards the ASP molecule, two structural analogues SA and BA (Figure 13) were selected as interfering substrates, in addition to ASP. The binding capacities are shown in fig.15. The nanostructured MIP had maximum binding capacity for ASP molecule as compared with bulk MIP owing to the increased number of specific binding sites on the surface of

IJSER

MWCNT-MIP whereas the adsorption capacity of non-imprinted polymers towards aspirin was lower than that of both imprinted polymers. NIPs bind compounds only by non-specific adsorption [20] due to the lack of formation of complimentary three-dimensional spaces in the polymer matrix which led to its decreased adsorption capacity than the MIPs. Also, the adsorption capacities of all four sorbents were found to be almost comparable for the structural analogs SA and BA due to the lack of structure specific cavities for the interfering compounds. These results suggested that depending on the interaction, size, shape and functionality of the template [21], the molecular imprinting process created a micro-environment in the polymer matrix. Table 3 summarizes the values obtained for distribution coefficient (K_d), selectivity coefficient (k) and relative selectivity coefficient (k').

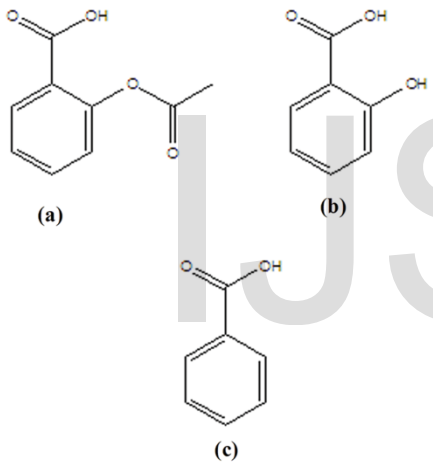

Fig. 13 Chemical structures of (a) ASP, (b) SA, and (c) BA

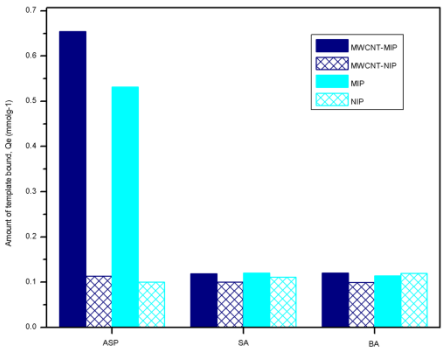

Fig. 14 Evaluation of the selectivity of MWCNT- MIP compared with MIP and both NIPs for ASP, SA and BA

Regeneration and reusability

The reusability of the regenerated molecularly imprinted polymers was studied about six sequential adsorption-desorption cycles (Figure 15). The MIPs were regenerated from all the rebinding studies using chloroform as solvent. The experiment showed that after six adsorption-regeneration cycles the regeneration capacity of MWCNT-MIP slightly decreased but not perceptibly. This may be attributed to the destruction of some recognition sites in the polymer matrix during the time of rewashing, and thus, were not fit for the template molecules anymore. The bulk MIP showed irregular trends of regeneration from the second cycle onwards because of the entrapment of template molecules inside the bulk thereby making it entirely difficult to leach out the template from the bulk during the regeneration process. In addition the destruction of some recognition sites owing to the reduced robustness of the non-nano sorbents also led to reduced regeneration. Thus it was showed that the synthesized MWCNT-MIP is a better adsorbent for selective separation of aspirin from its structural analogues than the bulk MIP.

IJSER

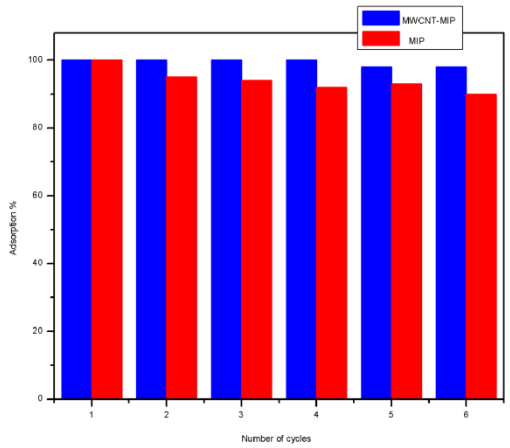

Fig. 16 Regeneration cycles of ASP onto MWCNT-MIP and MIP using chloroform as desorbing agent (Amount of polymer10mg; volume 8.0 mL; concentration of ASP 4mmolL^{-1},binding time 4h)

CONCLUSIONS

Artificial recognition surfaces on multiwalled carbon nanotubes for the selective and efficient separation of aspirin from its structural analogues were fabricated. The parameters affecting the rebinding of ASP by the synthesized sorbents were optimized and compared. The adsorption capacity was found to increase after the incorporation of MWCNT onto MIPs. The rate of kinetics of ASP adsorption was rapid in the case of MWCNT-MIP than the bulk MIP due to the availability of surface imprinted cavities. The well fit curve of Langmuir adsorption isotherm indicated a homogeneous distribution of binding sites with a monolayer adsorption of aspirin within the MWCNT-MIP matrix. The low cost, facile synthetic route and reusability of the nano-structured MIPs lend it a useful medium for ASP separation from its structural analogues such as SA and BA which was also confirmed by its high selectivity coefficient.

Conflict of Interest

The authors declare that no conflict of interest exists.

REFERENCES AND NOTES

[1] Arshady R and Mosbach K (1981) Synthesis of substrate-selective polymers by host-guest polymerization, Makromol Chem 182:687-692.

[2] Suedee R (2013) The Use of Molecularly Imprinted Polymers for Dermal Drug Delivery, Pharm Anal Acta 4:264-286.

[3] Huan Z, Yuzhi W, Chan N, Jinhuan K, Xiaojie L (2012) Preparation of magnetic molecularly imprinted polymers for separating rutin from Chinese medicinal plants, Analyst 137:2503-2512.

[4] Tian-Ying G, Yong-Qing X, Jin W, Mou-Dao S, Bang-Hua Z (2005) Chitosan beads as molecularly imprinted polymer matrix for selective separation of proteins, Biomaterials 26:5737-5745.

[5] Stephen PW, HienNguyen T, Paul G, Richard L, TongSun K, Grattan TV (2014) Preparation of novel optical fibre-based Cocaine sensors using a molecular imprinted polymer approach, Sens Actuators B 193:35-41.

[6] Haisheng Z, Weiping Z, Hongqing W, Yuyuan W, Fangfang H, Zhiqiang C, Honglin L, Jinhui T (2012) Selective Separation and Analysis of Pb(II) Using a New Surface Imprinted Multi-Walled Carbon Nanotubes Combined with AAS, J Anal Sci Methods Instrum 2:60-67.

[7] Cirillo G, Parisi OI, Curcio M, Puoci F, Iemma F, Spizzirri UG, Picci N (2010) Molecularly imprinted polymers as drug delivery systems for the sustained release of glycyrrhizic acid, J Pharm Pharmacol 62:577-582.

[8] Nicholas WT, Christopher WJ, Keith RB, Christopher JA, Vladimir H, David WB (2006) From 3D to 2D: A review of the molecular imprinting of proteins, Biotechnol Prog 22:1474-1489.

[9] Iijima S, (1991) Helical microtubules of graphitic carbon, Nature 354:56-58.

[10] Rezaei B and Rahmanian O (2012) Direct nanolayer preparation of molecularly imprinted polymers immobilized on multiwalled carbon nanotubes as a surface-recognition sites and their characterization, J Appl Polym Sci 125:798-803.

[11] Jianming P, Hang Y, Longcheng X, Hongxiang O, Pengwei H, XiuXiu L, Yongsheng Yan (2011) Selective Recognition of 2,4,6-Trichlorophenol by Molecularly Imprinted Polymers Based on Magnetic Halloysite Nanotubes Composites, J Phys Chem C 115:5440-5449.

IJSER

[12] Kan X, Geng Z, Zhao Y, Wang Z, Zhu JJ (2009) Magnetic molecularly imprinted polymer for aspirin recognition and controlled release, Nanotechnology 20:165601. doi: 10.1088/0957-4484/20/16/165601

[13] Pieter D, Dóra V, Yvan VH, Erwin A, Zsuzsanna K, Béla N, Désiré LM, Jobs H (2004) Characterisation of reversed-phase liquid-chromatographic columns by chromatographic tests comparing column classification based on chromatographic parameters and column performance for the separation of acetylsalicylic acid and related compounds, J Chromatogr A 1025:189-200.

[14] Jianfeng S, Yizhe H, Chen Q, Mingxin Y (2008) Layer-by-Layer Self-Assembly of Multiwalled Carbon Nanotube Polyelectrolytes Prepared by in Situ Radical Polymerization, Langmuir 24:3993-3997.

[15] Nanjundan AK, Hullathy SG, Jong SK, Yong SJ, Yeon TJ (2008) Preparation of poly 2-hydroxyethyl methacrylate functionalized carbon nanotubes as novel biomaterial nanocomposites Eur Polym J 44:579-586.

[16] Lagergren S (1898) Zur *theorie* der *sogenannten adsorption gelöster stoffe*, K Sven Vetenskapsakad Handl 24:1-39.

[17] Ho YS and McKay G (1998) The kinetics of sorption of basic dyes from aqueous solution by sphagnum moss peat, Can J Chem Eng 76:822-827.

[18] Bradley JC (2009) Lauren's Analysis of IR and HNMR Spectra for Aspirin. chem242. http://chem242.wikispaces.com/Lauren%27s+Analysis+of+IR+and+HNMR+Spectra+for+Aspirin. Accessed 25 February 2014

[19] Michael H Jnr and Ayebaemi IS (2005) Effects of temperature on the sorption of Pb^{2+} and Cd^{2+} from aqueous solution by Caladium bicolor (Wild Cocoyam) biomass, Electron J Biotechnol 8:162-169.

[20] Mathieu LN, Fatima P, Tobias Hey, Benoit G, Bo M (2007) Macroporous molecularly imprinted polymer/cryogel composite systems for the removal of endocrine disrupting trace contaminants, J Chromatogr A 1154:158-164.

[21] Ying L, Xin L, Cunku D, Yuqi L, Pengfei J, Jingyao Q (2009) Selective recognition and removal of chlorophenols from aqueous solution using molecularly imprinted polymer prepared by reversible addition-fragmentation chain transfer polymerization, Biosens Bioelectron 25:306-312.

IJSER